Electronic Supplementary Material (ESI) for Physical Chemistry Chemical Physics.
This journal is © the Owner Societies 2021

Microscopic interactions between ivermectin and key human and viral proteins involved in SARS-CoV-2 infection

Antonio Francés-Monerris,[a,b,*] Cristina García-Iriepa,[c,d,*] Isabel Iriepa,[c,e] Cécilia Hognon,[a] Tom Miclot,[a,f] Giampaolo Barone,[f] Antonio Monari,[a,*] and Marco Marazzi[c,d,*]

[a] Université de Lorraine and CNRS, LPCT UMR 7019, F-54000 Nancy, France.

[b] Departament de Química Física, Universitat de València, 46100 Burjassot, Spain.

[c] Departmento de Química Analítica, Química Física e Ingeniería Química, Universidad de Alcalá, Ctra. Madrid-Barcelona, Km 33,600, 28871 Alcalá de Henares, (Madrid), Spain.

[d] Instituto de Investigación Química "Andrés M. del Río" (IQAR), Universidad de Alcalá, 28871 Alcalá de Henares (Madrid), Spain.

[e] Departamento de Química Orgánica y Química Inorgánica, Universidad de Alcalá, Ctra. Madrid-Barcelona, Km 33,600, 28871 Alcalá de Henares (Madrid), Spain.

[f] Dipartimento di Scienze e Tecnologie Biologiche, Chimiche e Farmaceuticche, Università degli Studi di Palermo, Viale delle Scienze, 90128 Palermo, Italy.

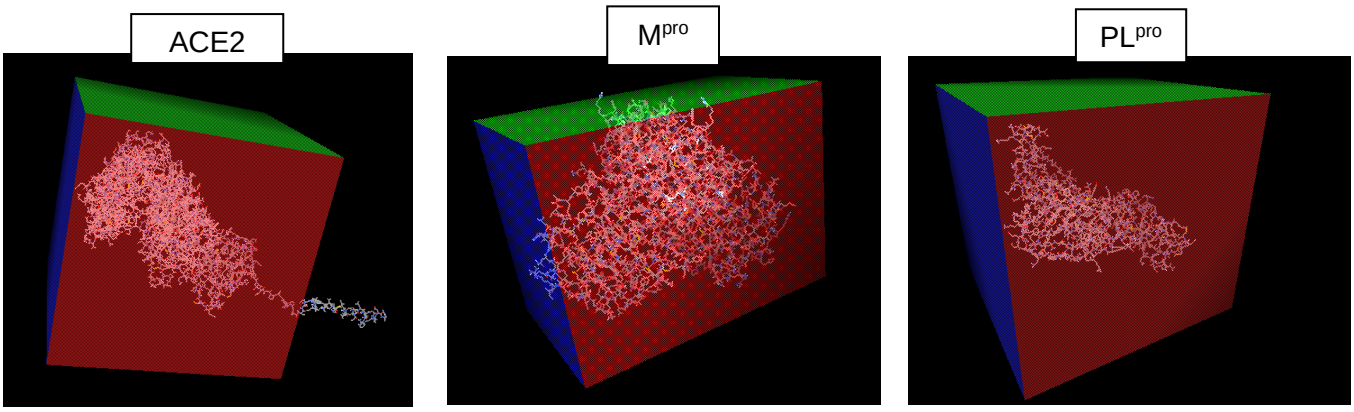

Figure S1. Grid-boxes for each investigated protein-protein/ligand complex.

Re-docking Study

a) ACE2

To evaluate the accuracy of the docking predictions, we first performed the molecular docking of the RBD fragment (from amino acid residues Phe486 to Tyr505 of the spike protein) in SARS-CoV-2, with the ACE2 receptor using the Auto Dock Vina software. Output poses generated were compared with the binding mode of the spike protein and ACE2 in the crystal structure complex (PDB ID 6M17, as already outlined in the Computational Methodology section). The mode of binding of ACE2 with the SARS-CoV-2 spike protein was structurally compared by superimposing both structures and evaluating its root mean square deviations (RMSD). The method is said to be valid if the RMSD value obtained is ≤2 Å, so that docking of the test compound can be carried out with the target protein in the same grid box area. The results indicated that the RMSD value obtained from the native ligand with the ACE2 receptor was 1.4723 Å.

b) $3CL^{pro}$

To validate the results, $3CL^{pro}$ was redocked. In this case, the receptor $3CL^{pro}$ (PDB ID: 6LU7) was docked to cocrystallized native ligand inhibitor N3 (N-[(5-methylisoxazol-3-yl) carbonyl]alanyl-L-valyl-N~1~-((1R, 2Z)-4-(benzyloxy)-4-oxo-1-{[(3R)-2-oxopyrrolidin-3-yl]methyl} but-2-enyl)-L-leucinamide). The docking results showed a RMSD value from the N3 ligand and $3CL^{pro}$ receptor of 1.2762 Å.

c) PL^{pro}

For PL^{pro} we used the only available crystal structure when we started this study (April 2020), which did not include any ligand (PDB ID: 6W9C). We are aware that in the meanwhile additional crystal structures of PL^{pro} complexed to various ligands have been published. Hence, in order to validate as first the chosen protein structure, we have superimposed the crystal structure of PL^{pro} in complex with the GRL0617 ligand (PDB ID: 7CJM) with the PL^{pro} crystal structure selected in this study (PDB ID: 6W9C), finding almost a structural match (RMSD value of 0.8404 Å). Therefore, we carried out the redocking of the ligand GRL0617 with the receptor 7CJM in the same grid box area and coordinates used for 6W9C. The RMSD value was 0.4991 Å, again validating our docking strategy.

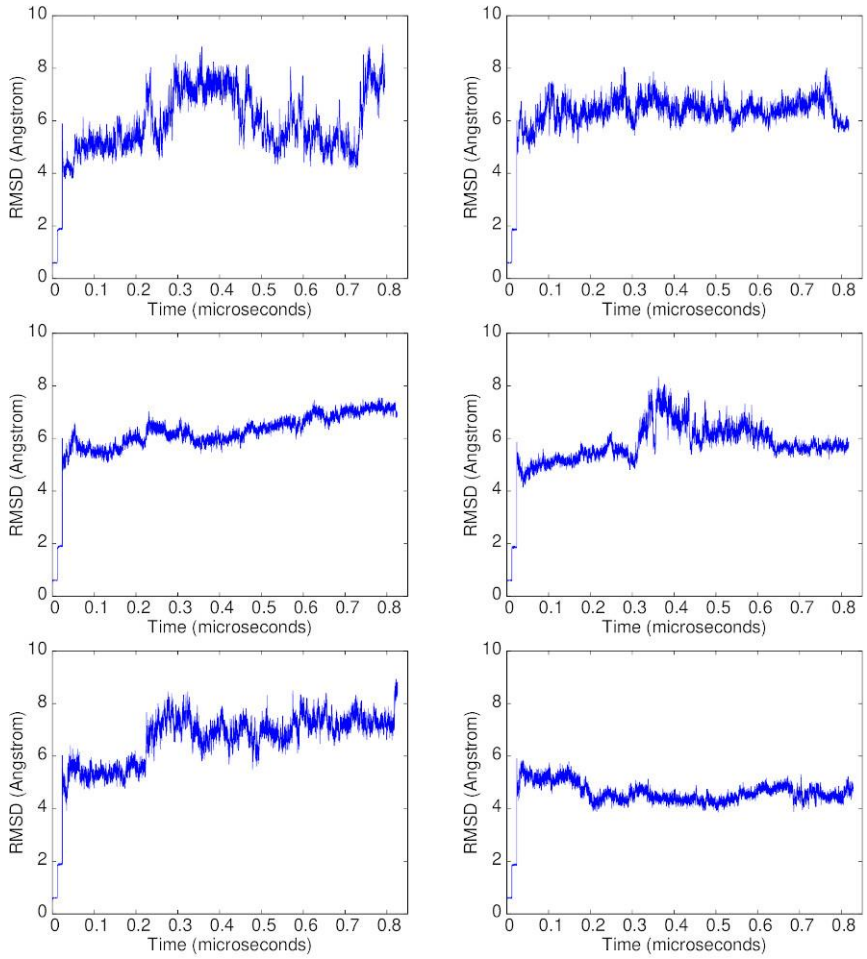

Figure S2. RMSD evolution of the ACE2 protein in the ACE2/IVE runs corresponding to interface-α-1 (top left), α-2 (top right), α-3 (center left), α-4 (center right), β-1 (bottom left), β-2 (bottom right). In all cases, the first 36 ns correspond to the system equilibration making use of harmonic constraints (*k*) at the protein backbones (12 ns with *k* = 1, 12 ns with *k* = 0.5, 12 ns with *k* = 0.1). Later, the constraints are completely released.

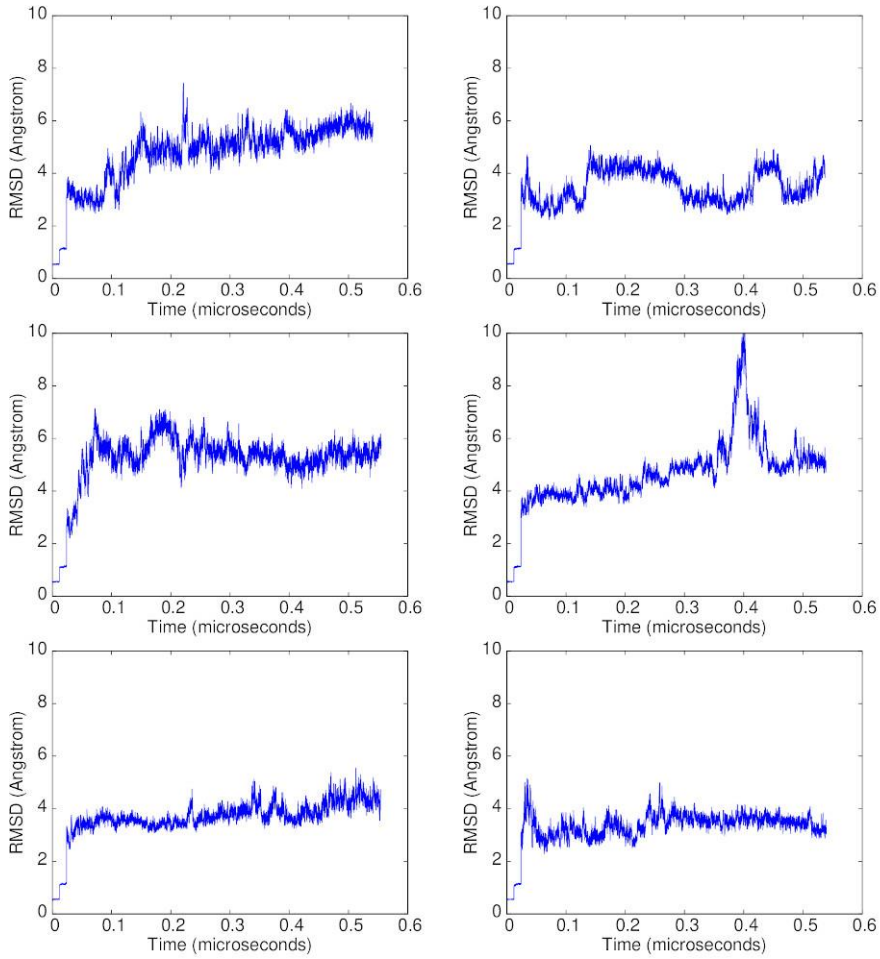

Figure S3. RMSD evolution of the ACE2 protein in the ACE2/IVE/RBD runs corresponding to interface-α-1 (top left), α-2 (top right), α-3 (center left), α-4 (center right), β-1 (bottom left), β-2 (bottom right). In all cases, the first 36 ns correspond to the system equilibration making use of harmonic constraints (*k*) at the protein backbones (12 ns with *k* = 1, 12 ns with *k* = 0.5, 12 ns with *k* = 0.1). Later, the constraints are completely released.

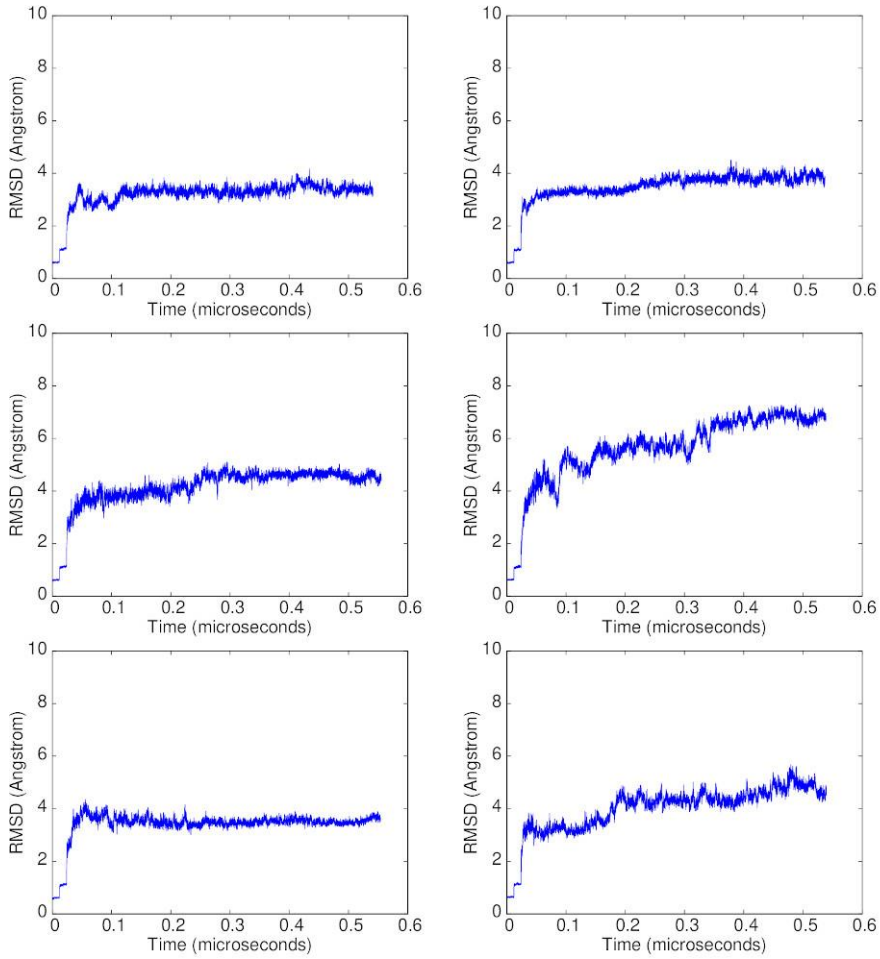

Figure S4. RMSD evolution of RBD in the ACE2/IVE/RBD runs corresponding to interface-α-1 (top left), α-2 (top right), α-3 (center left), α-4 (center right), β-1 (bottom left), β-2 (bottom right). In all cases, the first 36 ns correspond to the system equilibration making use of harmonic constraints (*k*) at the protein backbones (12 ns with *k* = 1, 12 ns with *k* = 0.5, 12 ns with *k* = 0.1). Later, the constraints are completely released.

CPPTRAJ scripts used to analyze the distances between the PD (ACE2), IVE, and RBD units

- Analysis of the distances between the peptidase domain (PD) of ACE2 (amino acids 1-69, 333, and 335) and IVE in the ACE2/IVE system:

```
distance ACE2-IVE :1-69,333,335@C,CA,N :711 out ACE2-IVE.dat
```

- Analysis of the distances between the peptidase domain (PD) of ACE2 (amino acids 1-69, 333, and 335), IVE, and the interacting part of RBD (amino acids 858, 861, 862, 850, 848, 831, 830, 868, 778, 824, 873, 875, 880, 820, 824, 868) in the ACE2/IVE/RBD system:

```
distance ACE2-RBD :1-69,333,335@C,CA,N
:858,861,862,850,848,831,830,868,778,824,873,875,880,820,824,868@C,CA,N out ACE2-RBD.dat

distance ACE2-IVE :1-69,333,335@C,CA,N :894 out ACE2-IVE.dat

distance RBD-IVE :858,861,862,850,848,831,830,868,778,824,873,875,880,820,824,868@C,CA,N :894
out RBD-IVE.dat
```

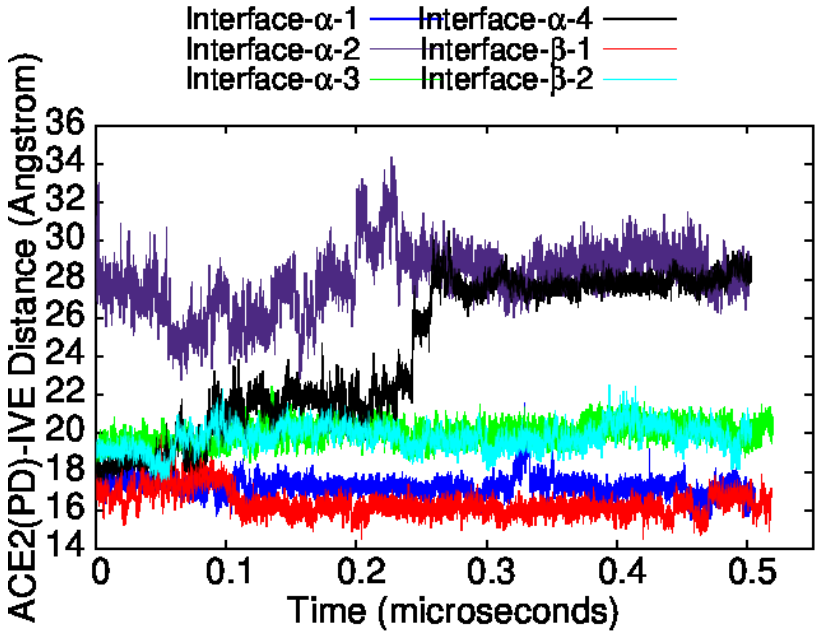

Figure S5. ACE2/IVE/RBD system. Evolution of the distances between the center of mass of the ACE2 PD (ochre amino acids in Figure 3A) and ivermectin.

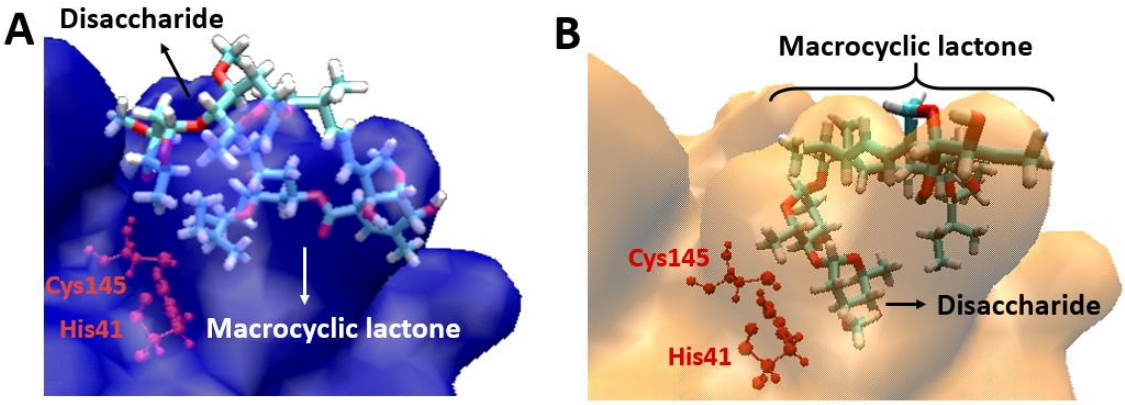

Figure S6. Representative poses of two ivermectin conformations inside $3CL^{pro}$ binding pocket with A) the disaccharide moiety out and B) deep inside the pocket.

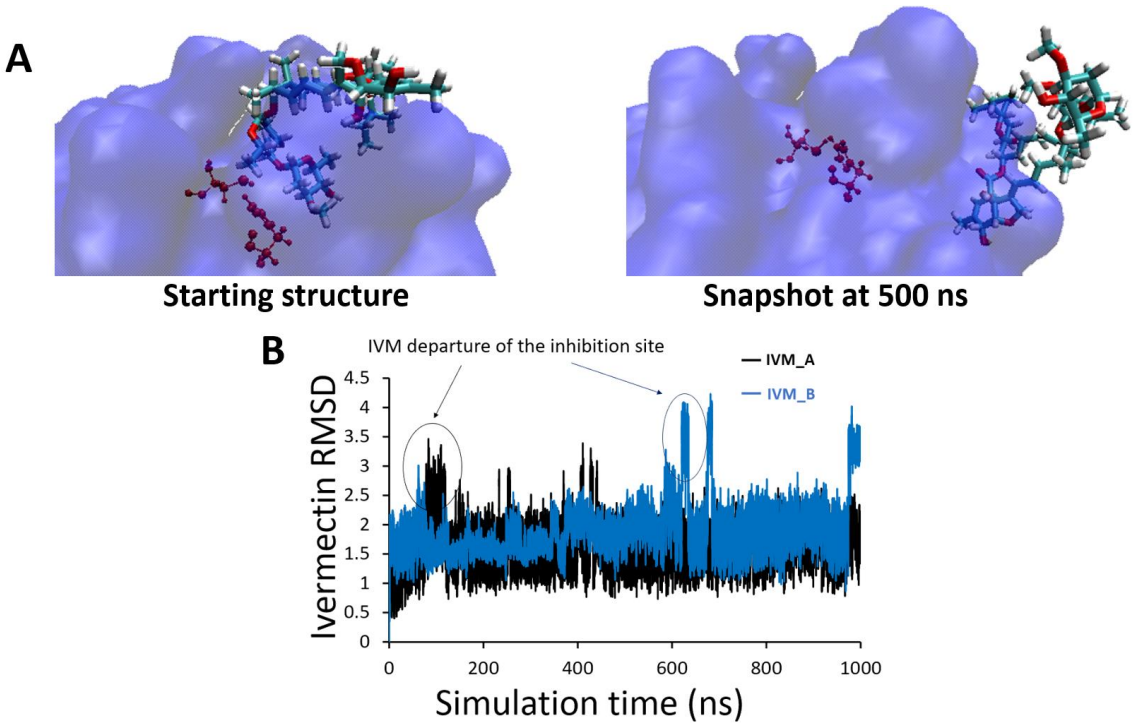

Figure S7. A) Starting and final snapshots of the MD simulation in which ivermectin starts with the disaccharide moiety inside the binding pocket but later moves outside, interacting with the $3CL^{pro}$ surface. B) Ivermectin RMSD plot showing that around 100 ns the RMSD of ivermectin interacting with chain A (IVM_A) significantly increases, matching with the time when it moves outside the pocket.

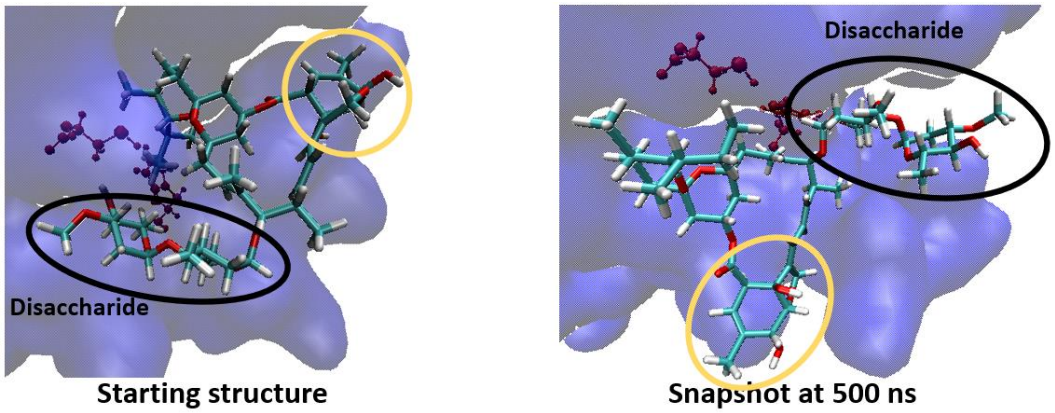

Figure S8. Upper view of $3CL^{pro}$ binding pocket, showing that when starting with the disaccharide moiety of ivermectin pointing outwards the pocket, ivermectin rotates on the surface along the MD simulation, as shown with the snapshot taken at 500 ns.

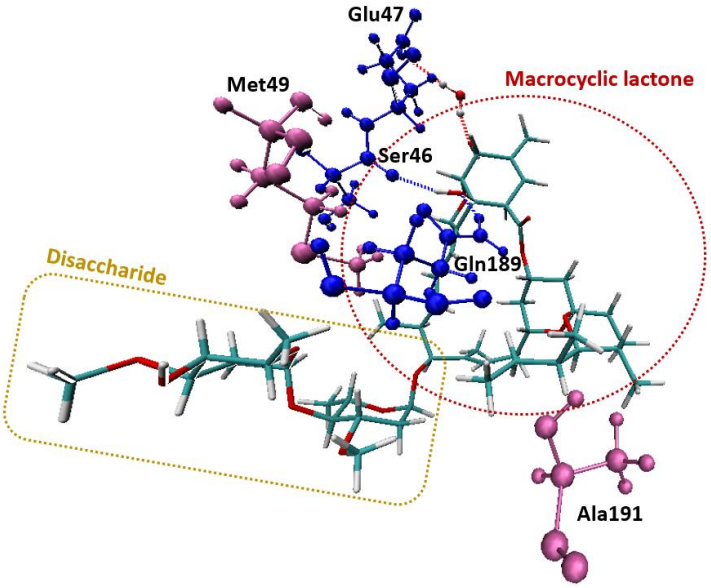

Figure S9. Scheme showing the amino acids leading to hydrogen-bond (in blue) or hydrophobic (in purple) interactions with the macrocyclic lactone moiety of ivermectin.

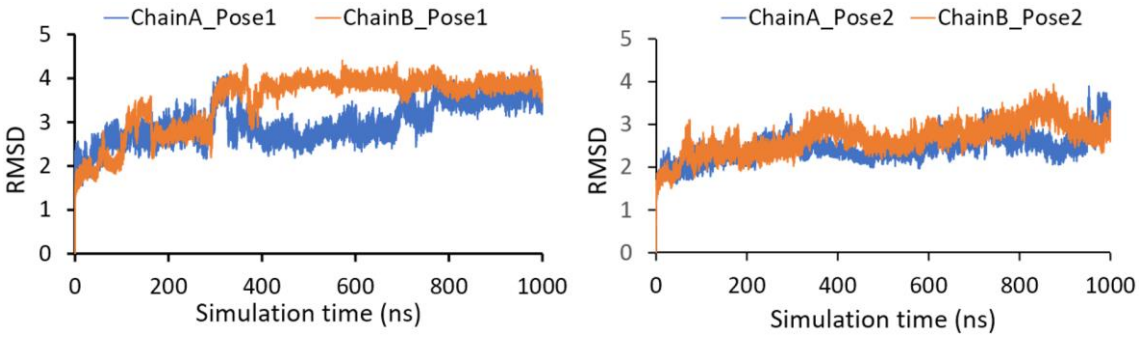

Figure S10. RMSD plots computed along the simulation time of the two independent MD simulations of the $3CL^{pro}$ dimer complexed with two ivermectin molecules.

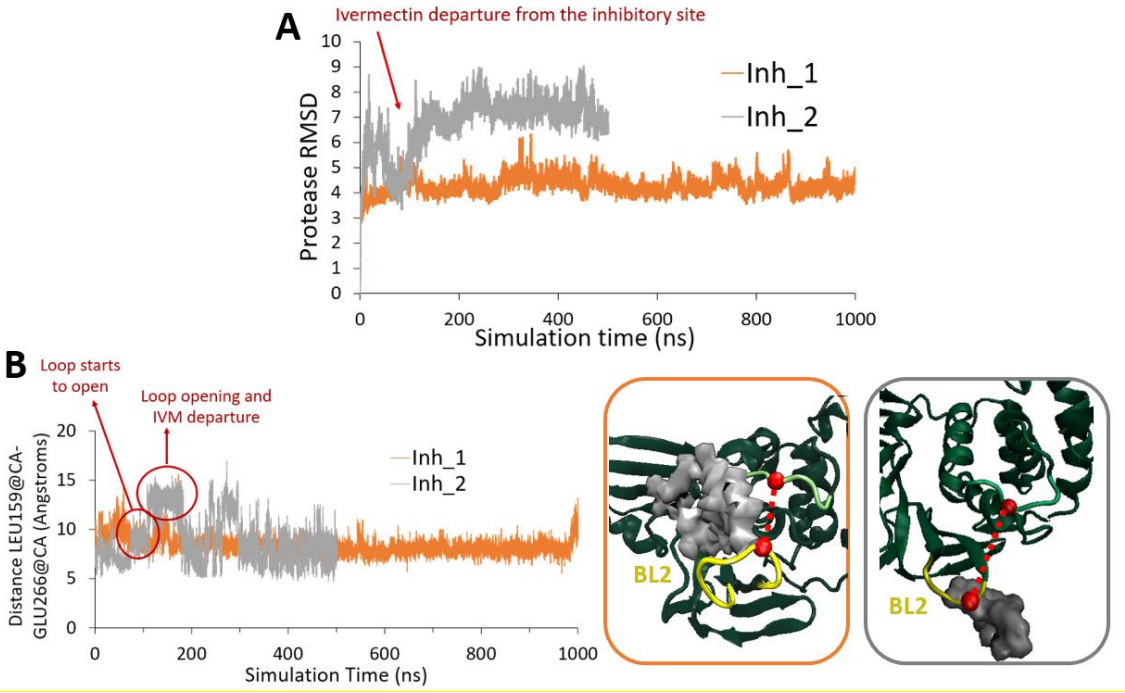

Figure S11. A) PL^{pro} RMSD plot for two independent MD simulations. B) Plot of the distance between one amino acid of the BL2 loop and one amino acid of the protease (depicted by two red balls and dotted line). Short distances indicate that the BL2 is closed while larger distances indicate its opening.

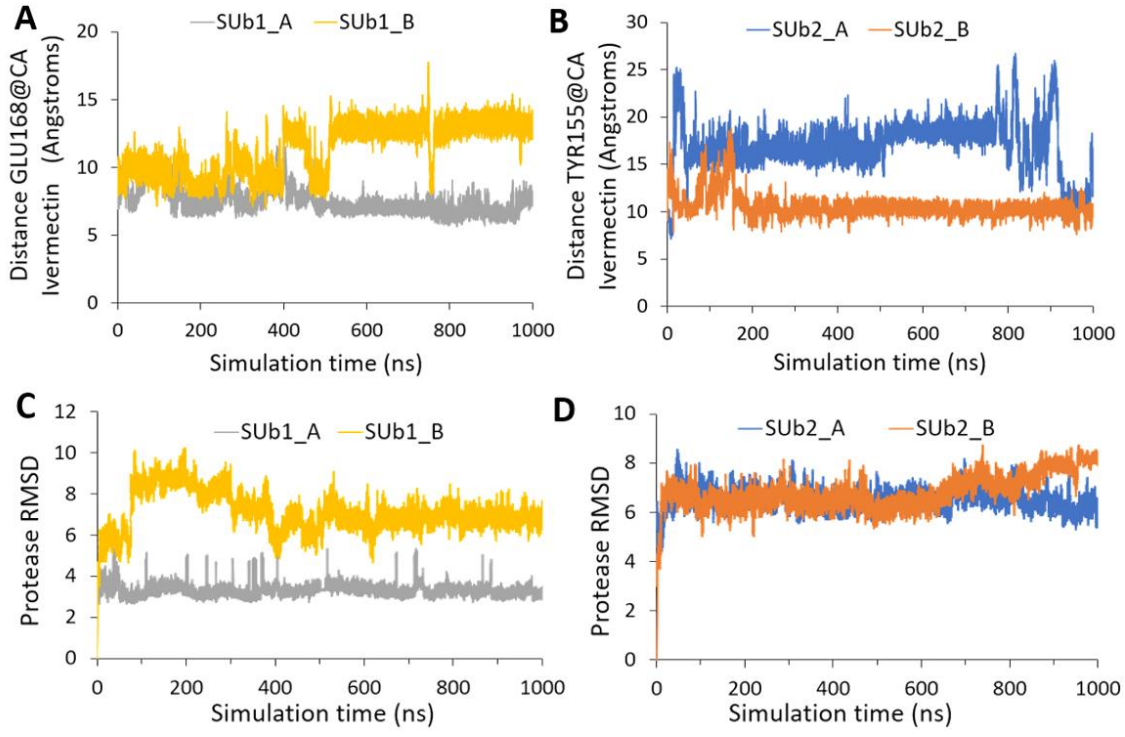

Figure S12. A) Ivermectin-GLU168 (residue located in the Sub1 domain) along the two MD simulations performed. B) Ivermectin-TYR155 (residue located in the Sub2 domain) along the two MD simulations performed, showing that for Sub2_B around 300 ns a stable conformation of ivermectin is reached. PL^{pro} RMSD plot for the simulations performed with ivermectin in the C) SUb1 and D) SUb2 domains.

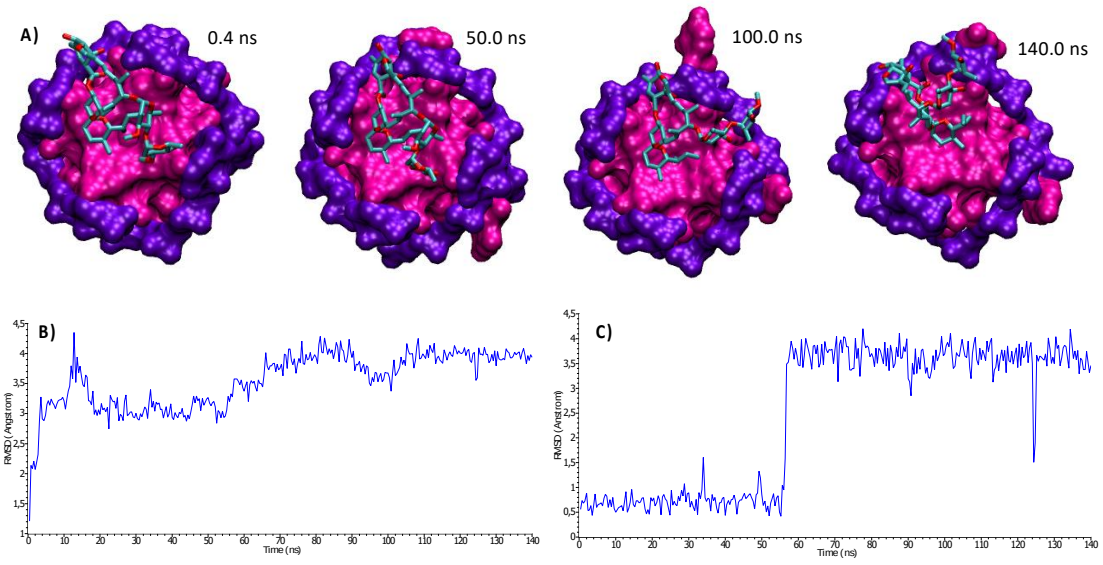

Figure S13. G4/IVE system (starting at G4 tetrad, left image). A) Representative snapshots of ivermectin interacting with the G4 RNA extracted from the MD simulation and showing the persistence of the aggregate with the tetrad. Total (B) and ivermectin (C) RMSD all along the MD simulation.

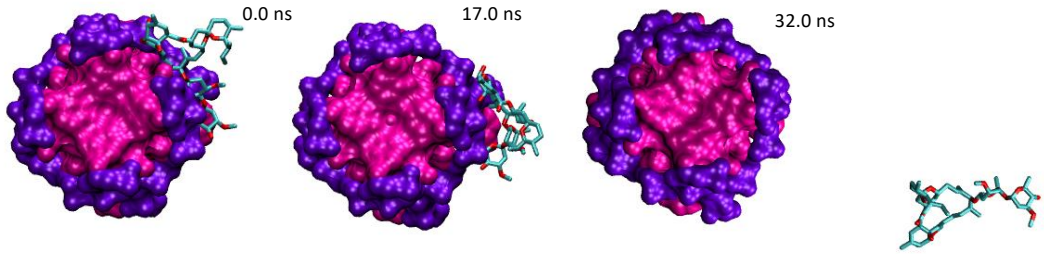

Figure S14. G4/IVE system (IVE starting at G4 backbone, left image). Representative snapshots of ivermectin interacting with the G4 RNA in the groove arrangement extracted from the MD simulation. The images show the instability of this interaction mode, that is detached after 32 ns.

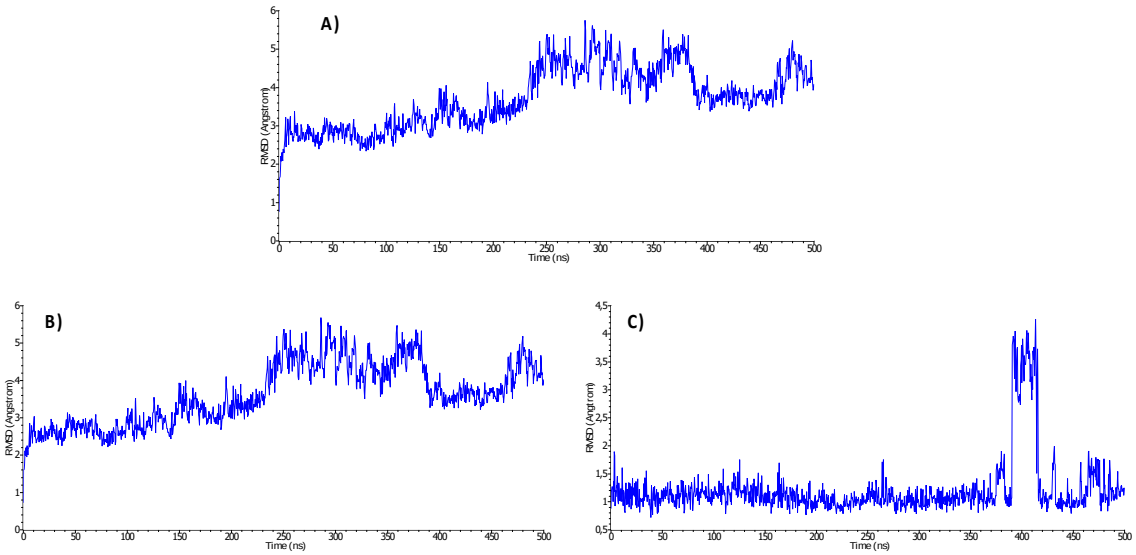

Figure S15. SUD/IVE system. Total (A) and partial RMSD for SUD (B) and ivermectin (C) all along the MD simulation. In C), the peak at *ca.* 400 ns corresponds to a temporary conformational change of IVE as a consequence of its flexibility.

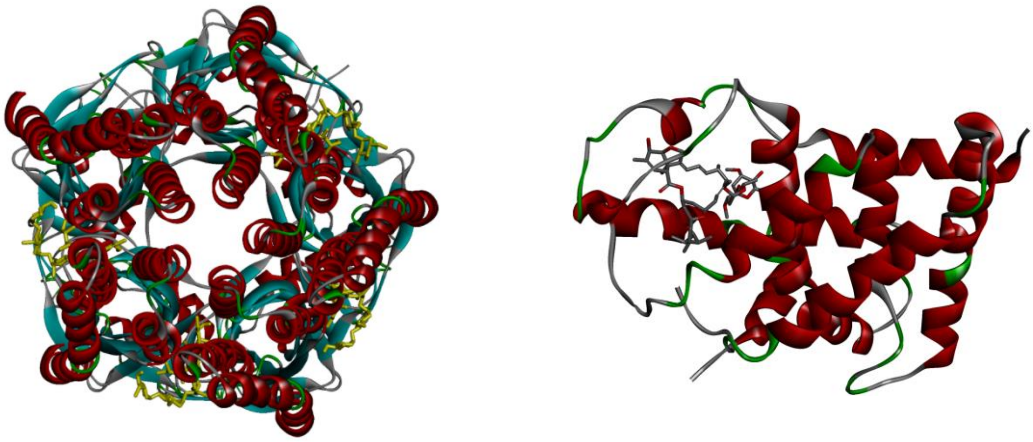

Figure S16. Left: IVE (in yellow) docked to four of the five *h*GlyR subunits. Right: IVE docked to *h*FXR.